Prospects for AGN Science using the ART-XC on the SRG Mission

Douglas A. Swartz[1], Ronald F. Elsner[2], Mikhail V. Gubarev[2], Stephen L. O'Dell[2], Brian D. Ramsey[2], Massimiliano Bonamente[3]

[1]Universities Space Research Association, NASA/MSFC [2]Space Science Office, NASA/MSFC [3]Department of Physics, University of Alabama Huntsville

The enhanced hard X-ray sensitivity provided by the Astronomical Röntgen Telescope to the Spectrum Röntgen Gamma mission facilitates the detection of heavily obscured and other hard-spectrum cosmic X-ray sources. The SRG all-sky survey will obtain large, statistically-well-defined samples of active galactic nuclei (AGN) including a significant population of local heavily-obscured AGN. In anticipation of the SRG all-sky survey, we investigate the prospects for refining the bright end of the AGN luminosity function and determination of the local black hole mass function and comparing the spatial distribution of AGN with large-scale structure defined by galaxy clusters and groups. Particular emphasis is placed on studies of the deep survey Ecliptic Pole regions.

Model Inputs & Assumptions

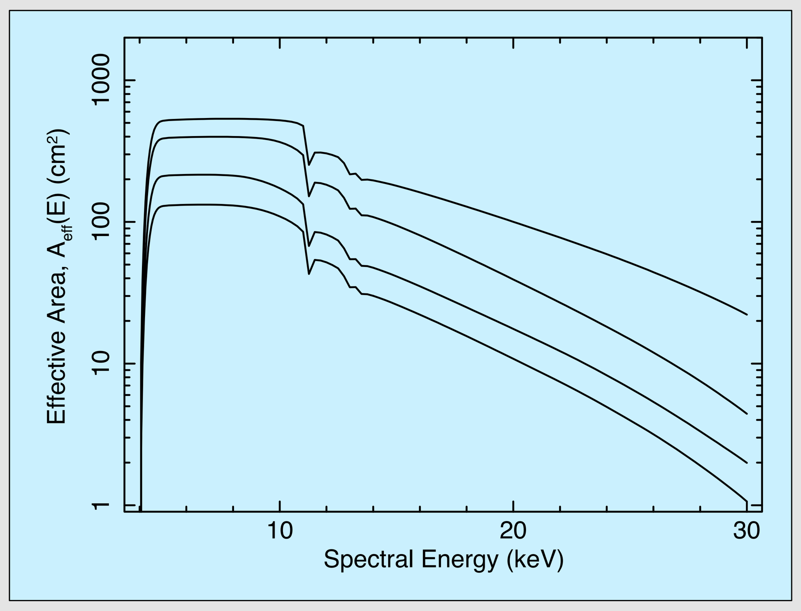

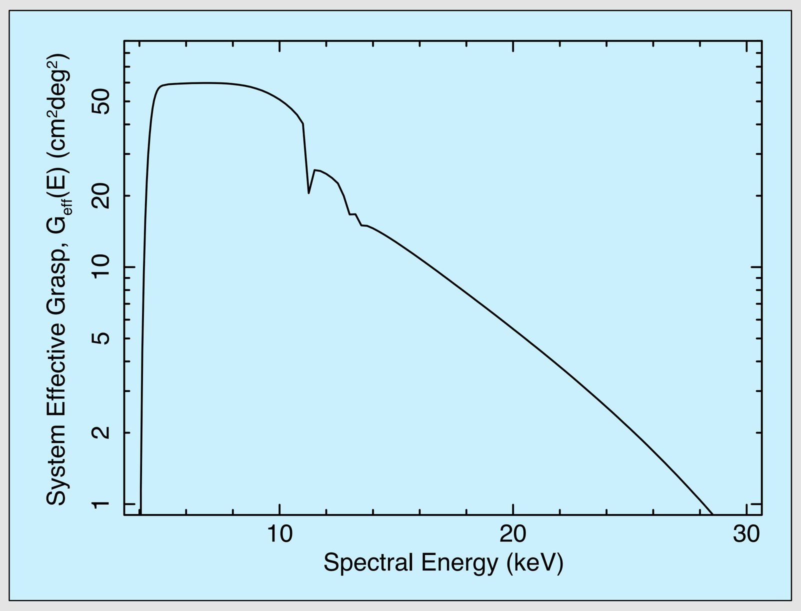

Optics & Detector Characteristics

The calculated ART-XC effective area, $A_{eff}(E,\theta)$, as function of energy, E, for four off-axis angles, θ = 0, 5, 10, and 15 arcmin, is shown in the left hand panel above. The system effective grasp $G_{eff}(E)$, using a 28×28 arcmin^2 detector field of view, is shown in the right panel. The effective grasp, which is the field-averaged effective area times the solid angle of the detector, is the most appropriate parameter for characterizing the survey sensitivity of ART-XC. In addition to the mirror configuration, the calculations of both $A_{eff}(E,\theta)$ and $G_{eff}(E)$ account for the quantum efficiency of the CdTe detector which has a strong cut-off below E ~5 keV but rapidly approaches 100% at higher energies.

CAN ADD MORE HERE AS NEEDED

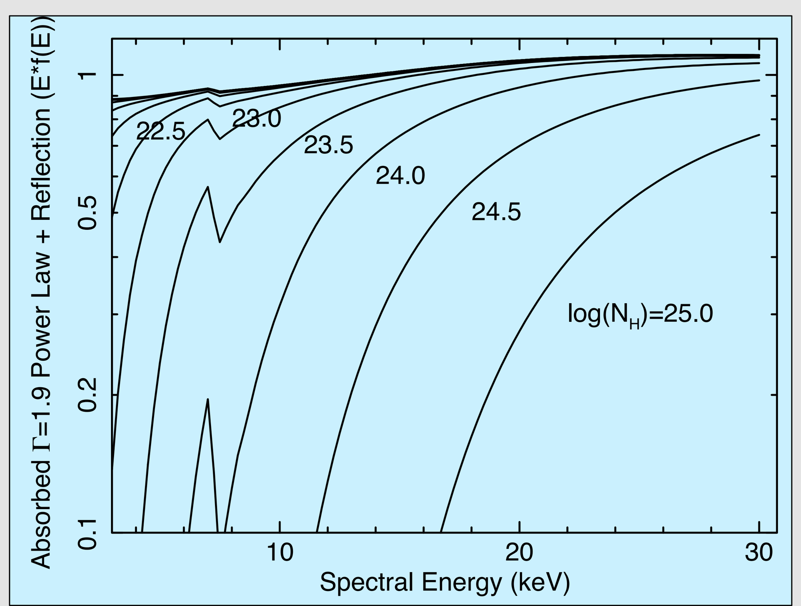

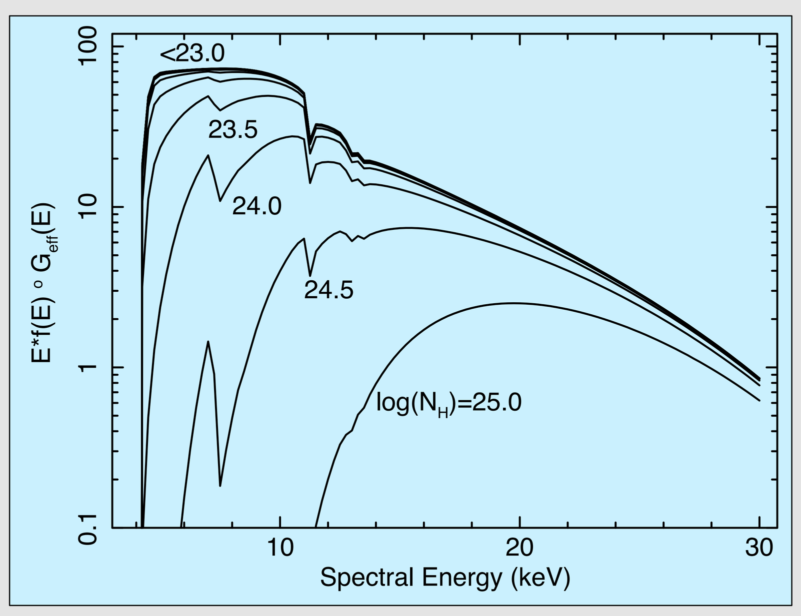

Model AGN Spectra

Active Galactic Nuclei (AGN) X-ray spectra are represented by an exponentially cut-off power law (Γ=1.9) attenuated by an intrinsic column density plus a contribution from emission reprocessed by the accretion disk using the Compton reflection model of Magdziarz & Zdziarski (1995) and model parameters from Gilli et al. (2007). These spectra are shown in the above left panel for several values of the attenuating column density, N_H. The spectra convolved with the effective grasp, $G_{eff}(E)$, of the ART-XC optics+detector are shown in the right panel.

Other Spectral Model Ingredients

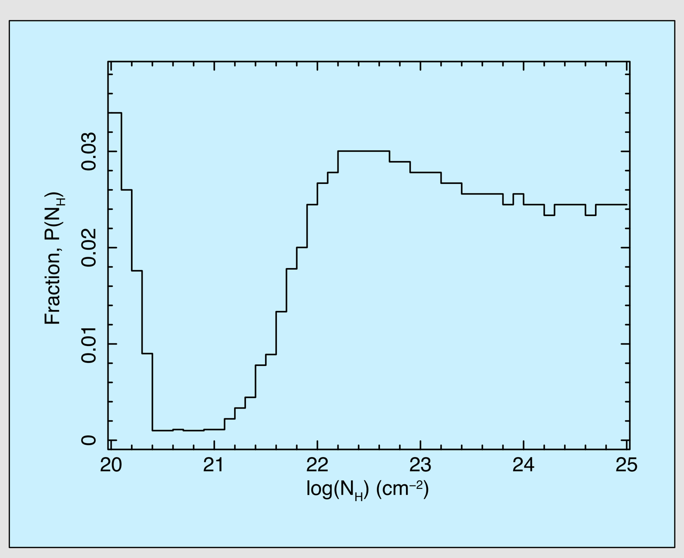

In addition to AGN X-ray spectra, our sensitivity calculations also require the distribution of intrinsic AGN column densities. We assume a simple dust torus based on the unified AGN model in which the geometrical parameters give the correct ratio of obscured to unobscured AGN consistent with observations of AGNs in the local universe following Treister & Urry (2005). The N_H distribution, $P(N_H)$, is shown in the panel on the left.

Finally, a map of the exposure time as a function of sky position (right, shown in a Mercator projection), provided by Igor Lapshov (IKI), is used to determine average exposure times for the all-sky and the Ecliptic Pole survey regions. The approximate North Ecliptic Pole (NEP) region (~200 deg^2) is indicated by the white ellipse.

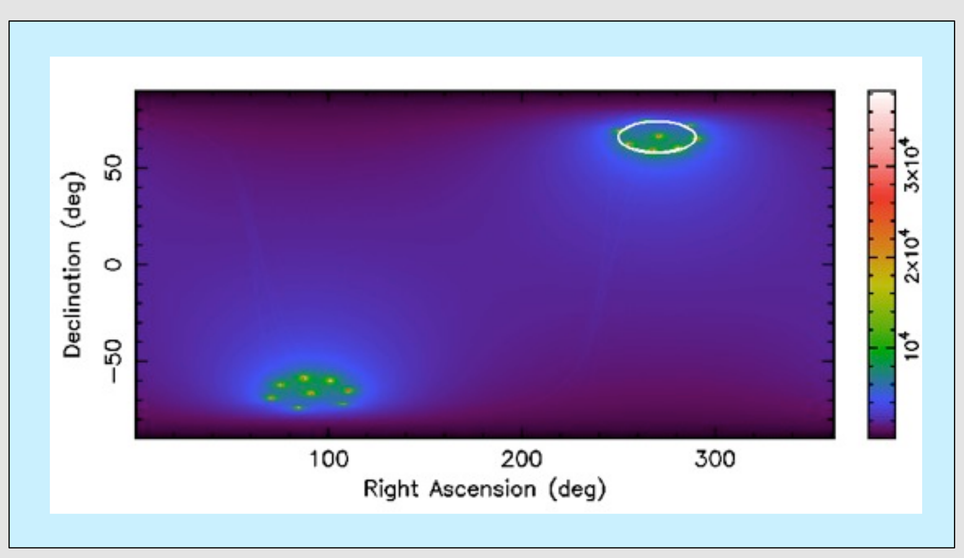

Sensitivity Calculation Results

Given an effective exposure time and specifying a minimum number of photons for detection, one can then calculate the sensitivity for the various AGN source spectra after convolving the source number spectrum with the effective exposure—i.e., with the field-averaged effective area times the time a given direction is in the detector's field of view. From these sensitivity calculations, the 2–10 keV log$N$–log$S$ relation of Moretti et al. (2003), and the distribution of intrinsic column densities in the simple unified AGN model, we estimate the total number of AGN detected in a survey and the number detected as a function of intrinsic column.

AGN Number Counts

The panel at right displays the differential number of sources per unit column density interval (lower curve) and the cumulative total number of AGN expected from the all-sky survey. The figure indicates that over 10,000 AGN will be detected including ~2500 moderate to highly obscured (N_H > 10^{23} cm^{-2}) sources. (The differential number of detected sources is low at N_H ~ 10^{21} cm^{-2} because of the paucity of AGN with low column densities in the unified model.) The differential and cumulative number distributions for the North Ecliptic Pole region are similar to those shown but scaled downward by a factor of ~100 because of the small sky area of the NEP even though the average exposure time there is ~4 times deeper than the rest of the sky.

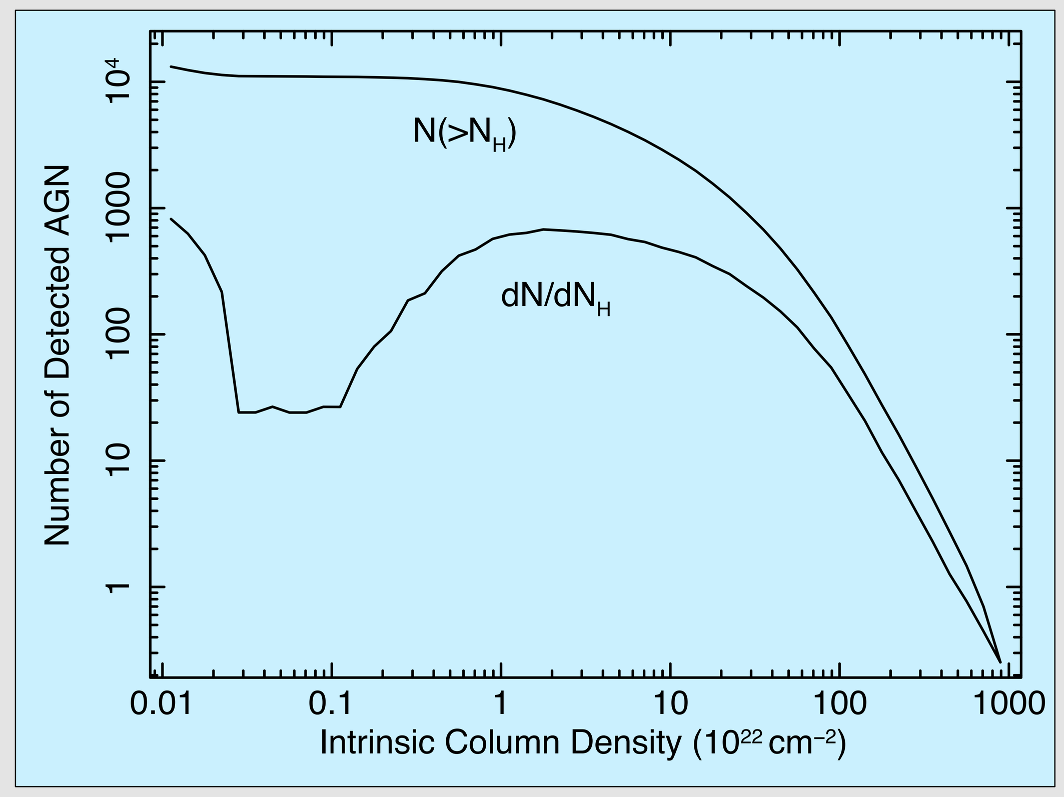

Cosmological Evolution

Most of the AGN sources detected by ART-XC in both the all-sky and Ecliptic Pole surveys will be local AGN. However, there is a non-negligible fraction of luminous AGN at cosmological redshifts that will also be surveyed. To estimate this population, we applied the luminosity-dependent density evolution (LDDE) model of Ueda et al. (2003). The panels below show (left) the 2–10 keV limiting flux, corresponding to a detection limit of 8 source counts, achieved by the ART-XC for the model AGN X-ray spectrum as a function of intrinsic column density at redshift z = 0; the differential 2–10 keV AGN luminosity function (center) shown as a function of observed flux rather than luminosity (cf., Fig. 11 of Ueda et al.); and the comoving spatial density of AGNs as a function of redshift for 3 luminosity ranges (right). This last panel shows that the peak density of the more luminous AGNs occurs at greater redshifts.

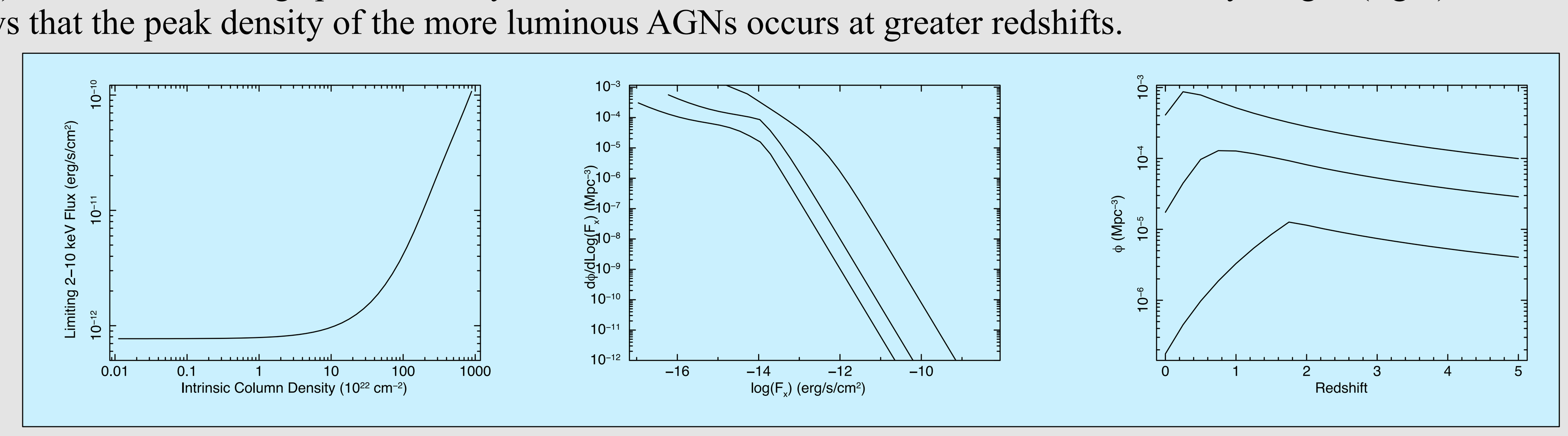

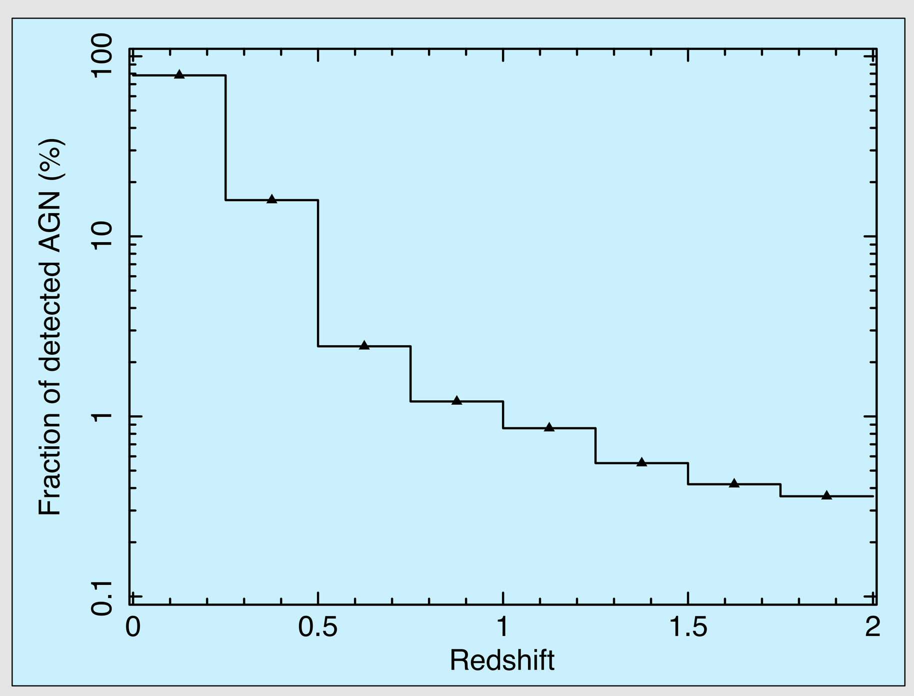

We can combine the above to determine the redshift distribution of AGN detected by ART-XC in survey mode as shown on the left. Here, the number of detected sources in each of several redshift bins out to z = 2 are accumulated and the fraction of detected sources in each bin calculated. To make this estimate, sources are assumed to be only mildly obscured so that the minimum detectable flux (after accounting for redshift of the source spectra) is ~8×10^{-13} erg/cm^2/s as shown in the left hand panel above as appropriate for N_H<10^{23} cm^{-2}.

References

Gilli, R., Camastri, A., & Hasinger, G. 2007, A&A, 463, 79
Magdziarz, P. \& Zdziarski, A.A. 1995, MNRAS, 273, 837
Moretti, A., Campana, S., Lazzati, D. & Tagliaferri, G., 2003, ApJ, 588, 696
Treister, E. \& Urry, C.M., 2005, ApJ, 630, 115
Ueda, Y., Akiyama, M., Ohta, K., & Miyaji, T., 2003, ApJ, 598, 886